ISSN: 2277-3754
ISO 9001:2008 Certified
International Journal of Engineering and Innovative Technology (IJEIT)
Volume 4, Issue 1, July 2014

Electromagnetic Emission Analysis for IC Packaging Structures

Nick K. H. Huang, Li Jun Jiang
khhuang@eee.hku.hk, jianglj@hku.hk
Department of Electrical and Electronic Engineering, The University of Hong Kong

***Abstract*—The IC packaging EMC/SI/PI problems have been broadly attested while its electromagnetic emissions are becoming increasingly significant as the data rate of digital system continues increasing. This paper focuses on EM emission behaviors for IC packaging structures. It is found that packaging EMI demonstrates clearly low and high frequency behaviors. Both theoretical analysis based on the first principle asymptotic forms and simulated results based on numerical full wave solvers are provided to investigate critical impacts to IC packaging EM radiation. It provides a basic modeling for comprehensive radiation studies. All modeling analysis in this paper contributes to the low EMI design rule development.**

***Index Terms*—cavity mode, EMI, IC packaging, EM radiated emission, via trace radiation**

I. Introduction

Over the past decades, high I/O densities, climbing data rates, and shrinking package dimensions lead to significant parasitic problems in multilayer packages and PCBs. Efficient and accurate modeling techniques for IC packaging optimization are essential for signal/power integrity (SI/PI) and electromagnetic compatibility/interference (EMC/EMI). However, most research efforts have been focused on SI/PI [1]–[3]. An estimation of maximum radiated emissions from power planes and a heatsink on a PCB in a closed-form expression has been derived and discussed in [4]–[6]. EMI for IC packaging was not critical because its dimension was a very small fraction of the working wavelength. Hence, it was not an effective radiator. However, because of the increasing working data rate, EMI caused by or partially by the packaging is becoming more significant. It could easily generate radiations above the EMC/EMI regulation. This paper focuses on the IC packaging electromagnetic emission property modeling.

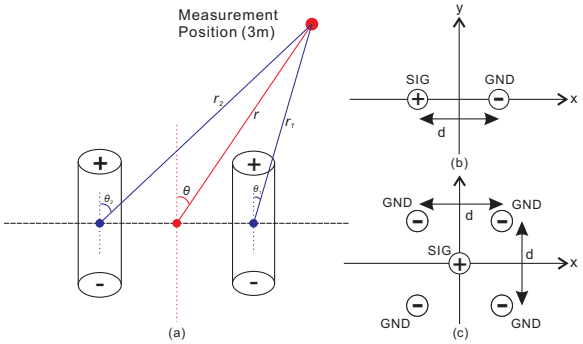

Figure 1. (a) Vias and the measurement position. (b) Two vias with opposite currents. (c) One signal via with four surrounding GND vias.

II. The Effects of Frequencies

The IC packaging structure is full of vias. Assume each via has the current I. Its current moment is $\mathbf{P} = I_0 dl\hat{\mathbf{a}}$, where $\hat{\mathbf{a}}$ is the unit vector of the via axis. Even though there are top and bottom ground planes, the via can still be asymptotically approximated by a Hertzian dipole as Fig. 1(a) when the frequency is low. Its radiated electric field (when placed at the origin) is

$$E_\theta = j\omega\mu\frac{I_0 dl}{4\pi}\cdot\frac{e^{-j\beta r}}{r}\cdot\sin\theta \tag{1}$$

Hence, $E_\theta \sim O(\omega)$. When there are two vias forming a current return path with opposite currents (see Fig. 1(b)), the total E-field is the result of multiplication of an array factor. At low frequencies,

$$E_\theta \approx j\frac{\omega^2\mu d}{c}\frac{I_0 dl}{4\pi}\cdot\frac{e^{-j\beta r}}{r}\cdot\sin\theta\cos\varphi \tag{2}$$

ISSN: 2277-3754
ISO 9001:2008 Certified
International Journal of Engineering and Innovative Technology (IJEIT)
Volume 4, Issue 1, July 2014

Hence, $E_\theta \sim O(\omega^2)$. When there are four GND vias symmetrically surrounding the signal via in Fig. 1(c), four GND vias are assumed to share the return current. At low frequencies,

$$E_\theta \approx j\frac{\omega^3 \mu d}{c^2}\frac{I_0 dl}{4\pi}\cdot\frac{e^{-j\beta r}}{r}\cdot\sin\theta\cdot\frac{d^2}{8}\cos^2(\varphi) \qquad (3)$$

Hence, $E_\theta \sim O(\omega^3)$. In general, the total E-field will increase at a rate of 20, 40, and 60 dB for one, two, and five via configurations, respectively.

The above analysis is only valid for low frequencies. If $d \approx 2$ mm, $\beta d \ll 1, \lambda_0 = 20\pi d$, we have $f_0 = {}^c/_{\lambda_0} \approx 2.39$ GHz. Hence, this analysis is invalid above 2.4 GHz. Beyond this frequency, the approximated dipole radiation mechanism is not accurate anymore. The effects of the top and bottom ground planes have to be considered. The parallel metal plates form cavities that support the cavity modes excited by vias. When the via distances are reduced, this limit frequency will increase. Hence, for packaging, this model could be useful for very high frequencies.

The emission tests at 3 meters for a parallel plate with different via configurations are shown in Fig. 2(a). It is observed that the radiated emissions are increasing approximately at the rate of 20 dB for one via, 40 dB for two vias, and 60 dB for five vias at frequencies below 2.39 GHz. It proves the proposed low frequency radiation models for vias in packaging. When vias are placed irregularly, the return currents will make the effective via configuration close to one of these three cases. Hence, at low frequencies, the increasing rate of the radiation shall be below 60 dB. More frequently, we shall see 20 dB increasing rate in practical implementations.

At high frequencies, the metallic cavity with dielectrics is dominated by TM^z cavity modes. TM^z modes' cutoff frequencies can be approximated by:

$$f_{TM^z_{mnp}} = \frac{1}{2\pi\sqrt{\mu\epsilon}}\sqrt{\left(\frac{m\pi}{a}\right)^2+\left(\frac{n\pi}{b}\right)^2+\left(\frac{p\pi}{c}\right)^2} \qquad (4)$$

where m, n, and p are integers, a, b, and c are the dimensions of the parallel plates. Similar equations can be obtained for TE^z modes. Physically TM^z modes shall be dominant in the layered packaging structure. Mathematically the lowest TE^z cutoff frequency is calculated to be above 100 GHz for the targeted structure, which is much higher than that of the first TM^z mode. The cutoff frequencies of TM^z modes when $p = 0$ are calculated and shown in Fig. 2(b). It reveals many correlations between the cutoff frequencies of cavity modes and the peak radiation of the packaging at frequencies between 3.5 and 20.5 GHz. It is also observed that the estimated cavity cutoff frequencies are not necessarily at the resonance. An imbalance difference model to calculate radiated emissions at resonant frequencies has been proposed and discussed in [7], [8].

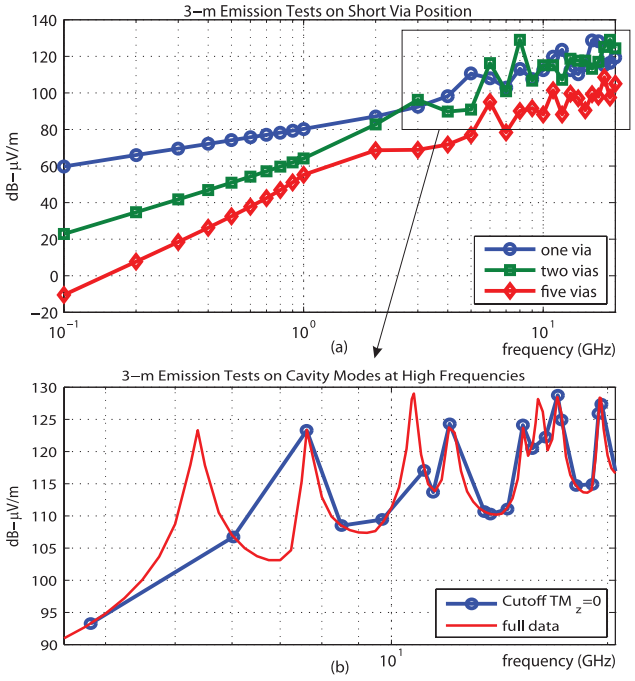

Figure 2. 3-m emission tests (a) for short vias and (b) cavity modes at high frequencies.

III. The Effects of Trace Structures

Traces are always connected with vias in packaging structures. Hence, it is interesting to know which one has bigger contribution to the radiated emission.

Two cases are studied and compared. Fig. 3(a) shows a trace in-between two shorted parallel plates. Both signal via and load via are surrounded by 4 GND vias that short top and bottom ground planes. In the second case shown in Fig. 3(b), the trace is removed. The vias are extended to plates. To maintain the same current on two vias, in Ansys HFSS the top surface of the via is used as the wave port, and the bottom surface of the via is used as the load. To compensate the phase shift due to the length of the trace, the excitation current phase of the right via in Fig. 3(b) has a phase delay equal to the phase shift of trace in Fig. 3(a) at each frequency. Both vias in Fig. 3(b) are extended by one time to enable reasonable port and load setups.

The simulated 3-meter radiated emissions of both cases at all frequencies are shown in Fig. 4. Two emissions are almost identical except a difference of around 6 dB. It means the radiated field magnitude of Fig. 3(b) is almost exactly doubled than that of Fig. 3(a). Considering the fact that the current

ISSN: 2277-3754
ISO 9001:2008 Certified
International Journal of Engineering and Innovative Technology (IJEIT)
Volume 4, Issue 1, July 2014

length of vias are doubled in Fig. 3(b), it is evident that the trace radiation is trivial compared to that of vias.

Here the conventional loop effect is not seen due to the symmetrical configuration and return current paths. Therefore, the loop effect is canceled out.

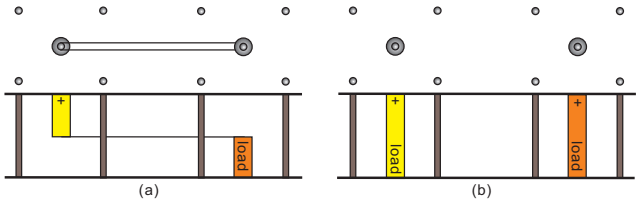

Figure 3. Trace EMI effect test by comparing two cases: with trace and without trace.

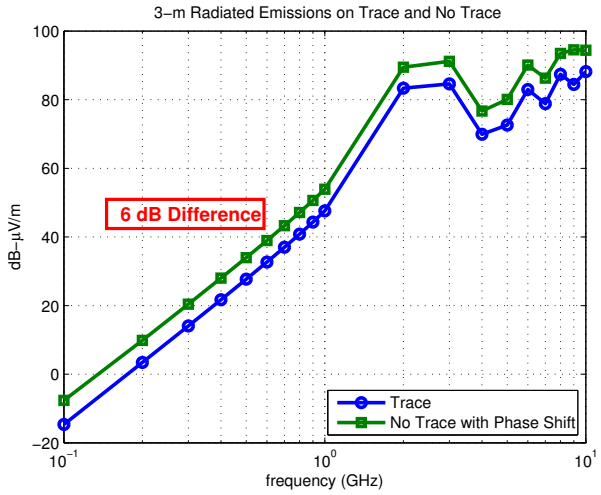

Figure 4. 3-m emission tests on trace and no trace.

The radiation patterns of both cases are shown in Fig. 5. They further prove that these two cases have the same radiation patterns at both low and high frequencies. The difference of each radiated pattern is also around 6 dB. However, this phenomenon only works for symmetrical striplines.

IV. The Position of the Stripline in the Package Layers

The position of a stripline is an important factor to the contribution of EMI. Figure 6 illustrates a stripline structure with different positions. Their radiated emissions are simulated at 3-meter measurement position. The first case has only one GND via next to the load as shown in Fig. 6(a). The whole structure supports a current loop around the top and bottom plates. The loop size is determined by the height h. The

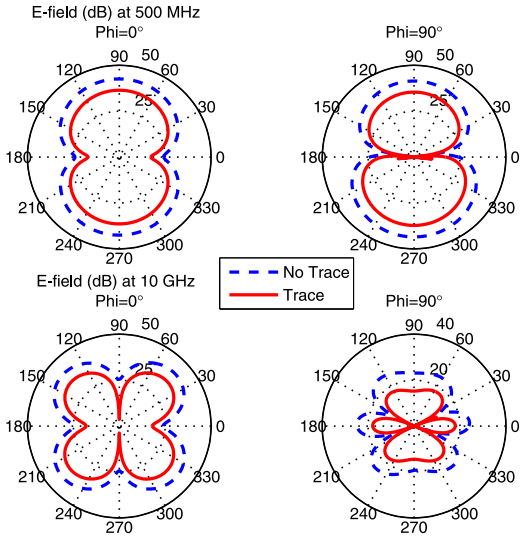

Figure 5. Radiation pattern of E-field (dB) with and without trace at 500 MHz and 10 GHz.

radiation results are shown in Fig. 7(a) for $h = H/5$, $H/2$, or $3H/4$, where H is the gap between two parallel plates. Apparently $H/5$ case has the lowest radiated emissions since it has the smallest current loop area. The highest radiation occurs in the case of $3H/4$ in Fig. 6 (a).

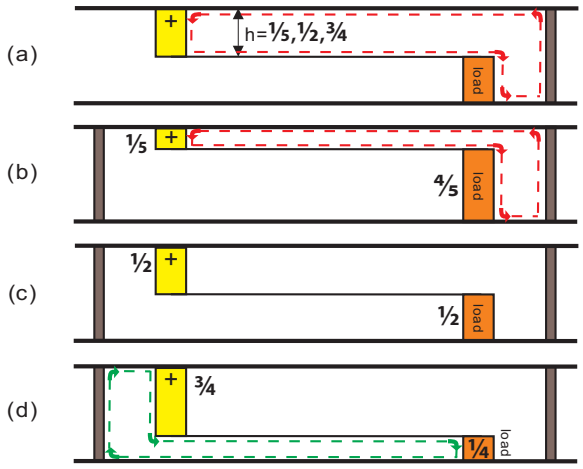

Figure 6. A stripline structure. (a) Cross-sectional view of the signal path with the trace h below the top plate for only one ground via at the right of the load. The signal path at height of (b) $H/5$, (c) $H/2$, (d) $3H/4$ for two ground vias.

The 2-GND-via structure is performed for three different trace positions with simulated results displayed in Fig. 7(b). Two loops are formed thus the overall radiated emissions are

ISSN: 2277-3754
ISO 9001:2008 Certified
International Journal of Engineering and Innovative Technology (IJEIT)
Volume 4, Issue 1, July 2014

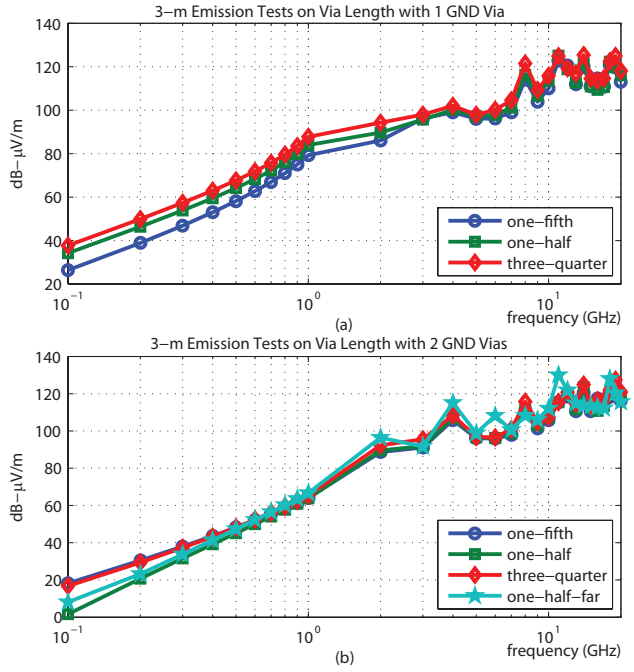

Figure 7. 3-m emission tests for (a) 1 GND via case and (b) 2 GND vias case.

less than one GND via cases because of flux cancellations. The lowest radiation happens when both loops have around the same areas to cause the balanced cancellation, which is the $H/2$ case. Another interesting point for the balanced $H/2$ case is to move the right GND via further away from the load via. Then the return current loop will become larger to cause unbalanced radiation for two current loops. Hence, higher radiated emissions (Fig. 7(b) last curve) is expected. It means when one GND via presents, a smaller loop area is preferred to cause less radiations. When two GND vias present, a balanced arrangement is preferred. But at very high frequencies, the radiation of all cases are similar. This tells that the cavity mode radiations become dominant.

V. Top-Layer Structures

When microstrip and CPW transmission lines are used on the top layer of the packaging, it is interesting to investigate their radiations. If many GND vias are added surrounding the trace and signal vias, the radiation would reach a saturation and the radiations of both cases are quite similar. Therefore, a two-layer simulation is performed to investigate the significance.

A. Differential-Line Effects

For CPW differential lines, the magnetic current plays an important role for radiated emissions. At the common mode, the magnetic current and electric field can be explained in Fig. 8 (a). The red arrow means the electric current flow, and G is the gap between the trace and the topside ground plane, where S is the spacing between two traces. $\mathbf{E}$ field is indicated by blue arrows, $\mathbf{M_s}(\mathbf{r})$ is the equivalent magnetic surface current on the artificial surface $\mathbf{M_s}(\mathbf{r}) = -\hat{\mathbf{n}}\times\mathbf{E}(\mathbf{r})$. Eqn. 5 shows the total $\mathbf{E}$ field caused by magnetic currents. The approximated total field is proportional to the summation of magnetic currents shown in Eqn. 6. Due to cancellation, the gap and spacing structures of differential CPW is not significant for the common mode.

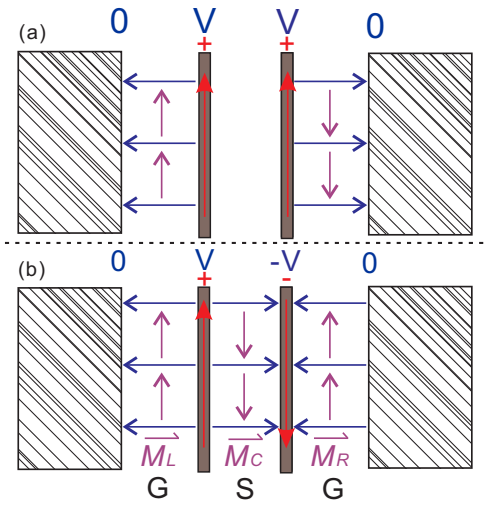

Figure 8. The differential CPW structure at (a) common and (b) differential modes.

$$\mathbf{E}_{total} = \mathbf{E}(\mathbf{M}_L) + \mathbf{E}(\mathbf{M}_C) + \mathbf{E}(\mathbf{M}_R) \tag{5}$$

$$|\mathbf{E}_{total}| \propto \frac{V}{G} + \frac{0}{S} - \frac{V}{G} \tag{6}$$

But for the differential mode, the electric currents are opposite to each other. Three magnetic current sources are present on gaps and the spacing. Similar to Eqn. 6, the total field is proportional to the source difference in Eqn. 7. The resultant conclusion is that when S is equal to G, the $\mathbf{E}$ field is minimum.

$$|\mathbf{E}_{total}| \propto \frac{2V}{S} - \left(\frac{V}{G} + \frac{V}{G}\right) \tag{7}$$

The common mode of CPW is very similar to a single line case. Narrower gap size reduces the radiations more because of less electric flux flowing to the air. However, there is no significant drop when we make the spacing equivalent to gap size. At differential mode shown in Fig. 9, when the spacing is set to the gap size, a noticeable reduction of radiations is

ISSN: 2277-3754
ISO 9001:2008 Certified
International Journal of Engineering and Innovative Technology (IJEIT)
Volume 4, Issue 1, July 2014

observed. In the last two cases, with the narrower gap, a greater reduction of radiations is attained. A further drop of 10 dB is achieved when the spacing is designed to be the same as the gap size. As a result, the magnitude of radiated emissions is inversely proportional to the gap size in CPW structures. A further decrease of radiations can be accomplished by setting the spacing to be the gap size for differential mode. This method minimizes the magnetic current and lower radiated emissions are expected. Similar ideas can be employed in three or even four lines of CPW structures.

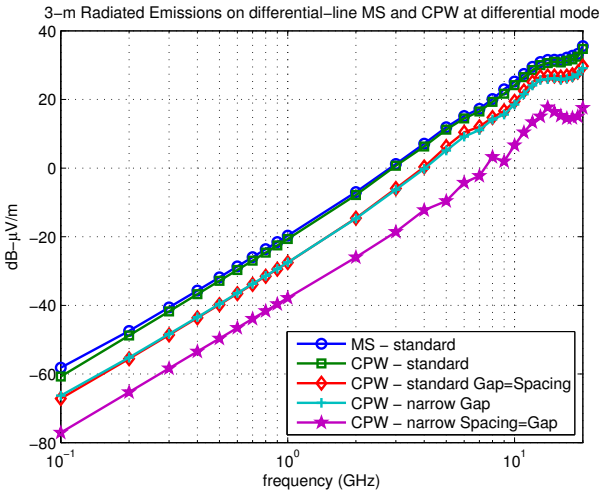

Figure 9. 3-m emission tests on differential-line microstrip and CPW at differential mode.

VI. Conclusion

This paper studies the fundamental principles and radiation mechanisms for IC packaging structures, a topic that was seldom addressed but is increasingly important recently. It tries to decompose contributions of key components to understand emission sources and critical parameters. Both theoretical arguments and supporting simulations based on the numerical full wave solver are provided to clarify significant impact factors to IC packaging EMI. It provides fundamental understandings and optimization guidelines for practical designs toward the packaging EMI reduction.

Acknowledgment

This work was supported in part by the Research Grants Council of Hong Kong (GRF 713011 and 712612), NSFC 61271158, and Hong Kong UDF Project.

References

[1] F. de Paulis, Y.-J. Zhang, and J. Fan, "Signal/power integrity analysis for multilayer printed circuit boards using cascaded s-parameters," *IEEE Trans. on EMC*, vol. 52, no. 4, pp. 1008–1018, nov. 2010.

[2] Y.-J. Zhang, Z. Z. Oo, X.-C. Wei, E.-X. Liu, J. Fan, and E.-P. Li, "Systematic microwave network analysis for multilayer printed circuit boards with vias and decoupling capacitors," *IEEE Trans. on EMC*, vol. 52, no. 2, pp. 401–409, may 2010.

[3] R. Rimolo-Donadio, X. Gu, Y. Kwark, M. Ritter, B. Archambeault, F. de Paulis, Y. Zhang, J. Fan, H.-D. Bruns, and C. Schuster, "Physics-based via and trace models for efficient link simulation on multilayer structures up to 40 ghz," *IEEE Trans. on MTT*, vol. 57, no. 8, pp. 2072–2083, aug. 2009.

[4] H.-W. Shim and T. Hubing, "A closed-form expression for estimating radiated emissions from the power planes in a populated printed circuit board," *IEEE Trans. on EMC*, vol. 48, no. 1, pp. 74–81, Feb 2006.

[5] H. Zeng, H. Ke, G. Burbui, and T. Hubing, "Determining the maximum allowable power bus voltage to ensure compliance with a given radiated emissions specification," *IEEE Trans. on EMC*, vol. 51, no. 3, pp. 868–872, Aug 2009.

[6] X. He and T. Hubing, "A closed-form expression for estimating the maximum radiated emissions from a heatsink on a printed circuit board," *IEEE Transactions on*, vol. 54, no. 1, pp. 205–211, Feb 2012.

[7] C. Su and T. Hubing, "Imbalance difference model for common-mode radiation from printed circuit boards," *IEEE Trans. on EMC*, vol. 53, no. 1, pp. 150–156, Feb 2011.

[8] C. Su and Hubing, "Calculating radiated emissions due to i/o line coupling on printed circuit boards using the imbalance difference method," *IEEE Trans. on EMC*, vol. 54, no. 1, pp. 212–217, Feb 2012.